The very early inflammatory triquetral lesion by magnetic resonance imaging – is this the first sign in rheumatoid arthritis?

Larios-Forte MC[1], García-Coronado JM[2], Skinner-Taylor CM[3], Esquivel-Valerio JA[3], Vega-Morales D[3], Vilchez-Cavazos F[4], Quiroga-Garza A[2], Elizondo-Omaña RE[2]

ACTA REUMATOL PORT. 2019;44:218-224

ABSTRACT

Introduction: Rheumatoid Arthritis (RA) an autoimmune, chronic, and disabling disease if untreated, affects wrist joints, with a diagnostic delay of up to 2 years. Triquetral bone allows rotational movement that pivots over the rest wrist bones, and maintains physiological loads during mobility. Magnetic resonance imaging (MRI) is the most sensitive (96%) method for diagnosis, shows lesions as early as in the initial RA stages. Our aim was to determine the most frequently affected structures in the hand-wrist joint by MRI using the OMERACT-RAMRIS Score (2003) in three different RA stages, including clinically suspicious arthralgia (CSA) that haven't reported before

Methods: We performed an exploratory, transverse, observational, descriptive study in 60 patients enrolled and classified by rheumatologists as: CSA, early rheumatoid arthritis (ERA), and established RA, prior to performing a dominant hand-wrist MRI for evaluation and descriptive analysis by an expert radiologist

Results: Female predominance 83% (50), with a mean age 42.0+/-13.5 years; A total of 1,731 hand-wrist bone and joint sites were evaluated using EULAR-OMERACT Atlas (2005), identifying 56% (964 sites) with typical RA lesions: synovitis, erosions, and bone marrow edema (BME or osteitis); synovitis was the most frequent with 46% (445 site-lesion), and triquetral synovitis the most frequent each clinical group: CSA 87% (20/23), ERA 91% (20/22), and RA 93% (14/15)

Conclusion: Synovitis and triquetral synovitis were the most prevalent lesion in three-studied phases. This could suggest the triquetrum as the first morphological site to be affected by RA; so it's assessment should be considered in the RA evaluation when it's clinically suspected.

Keywords: OMERACT-RAMRIS Score; Triquetrum bone; Magnetic Resonance Imaging; EULAR-OMERACT Atlas; Rheumatoid Arthritis.

1. Radiology and Research Division, Hospital Regional Monterrey, ISSSTE
2. Human Anatomy Department, Universidad Autonoma de Nuevo Leon, Facultad de Medicina
3. Rheumatology Department, Internal Medicine Division, Universidad Autonoma de Nuevo Leon, Hospital Universitario "Dr. José Eleuterio González"
4. Traumatology & Orthopedic Division, Universidad Autonoma de Nuevo Leon, Hospital Universitario "Dr. José Eleuterio González"

INTRODUCTION

Rheumatoid arthritis (RA) is the most common chronic autoimmune disease, characterized by joint destruction, disability, and life expectancy reduction due to progressive inflammatory complications[1]. Early diagnosis allows prompt treatment and reduces joint damage[2,3]. Magnetic resonance imaging (MRI) is the primary imaging study to visualize anatomical structures, abnormalities, variants, cortical bone shape irregularities, and morphological changes in RA according the American College of Radiology (ACR) Appropriateness Criteria[4]; it is the most sensitive (96%) diagnostic test and disease follow-up imaging method with a high specificity (94%) that can evidence pathologic hand-wrist lesions in initial RA phases. The European League Against Rheumatism-Outcome Measures in Rheumatology Clinical Trials (EULAR--OMERACT) Atlas (2005) and the OMERACT-RAMRIS Rheumatoid Arthritis Magnetic Resonance Imaging Score (2003) have established a Score Sheet for assessment with MRI[5-7].

Resnick (1976) wrote about ERA phase describing frequents erosions in the pisiform and triquetrum bones after synovial proliferation. Other studies have reported a relation between age and erosion lesions in

the carpal joint[8]. The hand-wrist complex is an anatomical joint structure that connects the radius-ulna distal joint to the proximal metacarpals. It possesses great ligament variability, capsules, and bone structures, each one with different functions. Carpal bones are joined by strong *intrinsic ligaments* (interosseous dorsal and radial ligaments with low flexibility) and *extrinsic ligaments* (palmar and dorsal), that maintains the biomechanics of the joint (physiological loads and the mobility arcs resistance), and provides wrist stability. These ligaments also have mechanoreceptors and provide proprioception and neuromuscular control, which predominate at the triquetrum bone, where most ligaments from the two carpals rows are inserted[9-11].

At the first carpal row, which has the most mobility, the scaphoid and triquetrum contribute to stabilize the central carpal column joint, allowing ample movements of flexion-extension and abduction-adduction (80% radial distribution and 20% ulnar)[4,11-13]. The triquetrum bone has a pyramid-shaped with 4 articular facets: the proximal, distal, lateral, and medial, articulating with the triangular fibrocartilage (first joint capsule), the hamate bone, the lunate bone, and the pisiform (second joint capsule) respectively. This articulated triangular fibrocartilage absorbs and transmits the forces and pressures exerted on carpal bones[12]. Its stability depends on nine palmar and dorsal interosseous ligaments with mixed fiber directions, joining all the carpal bones. The most morphologically controversial ligament according to Nozaki[14] is the ulnar collateral ligament (as Hogikyan and Louis described as well as Bogumill) which it's morphology includes to the pisiform bone[4,13,14] (Table I).

Some studies report in beginning early stages of RA, the triquetrum, capitate, and lunate bones are frequently affected with erosions[15-17]. Tamai *et al.*[18], (2007) reported by MRI in ERA, the relationship between bone marrow edema (BME or osteitis) and serological markers (C-Reactive Protein, Antibody-IL-6, anti-CCP [anti-cyclic citrullinated peptide], HLA-DRB1 and DAS-28 [Disease Activity 28 joints Score]) with their autoimmune, anatomical, and traumatic factors, that play an important role with synovial and erosions pathogenesis. These appear predominantly in the metacarpophalangeal areas (MCP), influenced by the location of the ligaments[18,19].

The aim of our study was to evaluate by MRI, patients from three different RA clinical stages, including the clinically suspicious arthralgia (CSA), to assess the starting structural changes and determine the most frequently affected site within the complex hand-wrist joint bones and topography.

MATERIALS AND METHODS

An exploratory, transverse, descriptive, non-blinded observational study, was performed in a northeastern Mexican cohort population (Monterrey, Nuevo Leon) from November 2016 to February 2017. Overall, 60 adult patients were enrolled from the rheumatology clinic (UANL University, School of Medicine), who accepted and signed informed consent; all assessed according to the American College of Rheumatology: ACR-EULAR (2010) criteria and were classified into three clinical groups, according to their RA phase (CSA, ERA, or RA). The CSA group included patients (RA direct relatives) with only arthralgia symptoms without clinically detectable inflammation, considered by the rheumatologists as being suspect to progress to arthritis over time; ERA group, consisted in patients with less than 2 years from the onset of arthralgia and joint inflammation, and the established RA patients group with more than 2 years with disease activity score (DAS28 greater than 2.6)

Simple T1 and STIR (Fat Sat - General Electric Signa Twin HDx 1.5 Tesla) MRI sequences were obtained from the dominant hand (Table II). One day prior to the study patients stopped anti-inflammatory medication. Images were evaluated by a musculoskeletal radiologist, according the EULAR-OMERACT (Outcome Measures in Rheumatoid Arthritis Clinical Trials) Atlas 2005 in order to identify the RA known lesions: synovitis, erosions, and BME/osteitis.

Descriptive statistics was performed with chi square test to differentiate between groups in SPSS (IBM *Statistical Package for the Social Science* SPSS, 22 version)

This study was reviewed and approved by the Ethics and Research Committees of the UANL University, School of Medicine: Registration number RE-17-00010, complying with the Helsinki Declaration.

RESULTS

A total of 60 MRIs were performed in patients with a mean age of 42.0+/-13.5 (19–70) years. Most were women 83% (50 women/10 men), and were distributed in 3 different RA stages as: CSA with 38% (23), ERA 37% (22), and RA 25% (15).

TABLE I. PROXIMAL CARPAL BONE LIGAMENT DISTRIBUTION

Bone	Lig	Location	Specification
Triquetrum	9	1 I	Lunotriquetral
		4 P	Long radiolunate (radiolunotriquetral), ulnotriquetral, capitotriquetral (triquetrohamocapitate), ulnar collateral
		4 D	Dorsal radiocarpal (dorsal radiotriquetral), dorsal intercarpal (dorsal scaphotriquetral), triquetrohamate (dorsal), scaphotriquetral
Scaphoid	7	2 I	Scapholunate, scaphotrapeziotrapezoid (palmar)
		4 P	Radioscaphoid (radial collateral), scaphocapitate, scaphotriquetral, radioscaphocapitate (palmar)
		1 D	Dorsal Intercarpal (dorsal scaphotriquetral)
Lunate	6	2 I	Scapholunate, lunotriquetral
		3 P	Long radiolunate (radiolunotriquetral), short radiolunate, ulnolunate
		1 D	Dorsal radiocarpal (dorsal radiotriquetral)
Pisiform	1	0 I	–
		0 P	–
		1 D	Ulnar collateral

Lig: Ligaments involving the carpal bone; I: Interosseous; P: Palmar; D: Dorsal.

TABLE I. MAGNETIC RESONANCE HAND PROTOCOL

Sequences	TR/TE (msec)	Slice Thickness (mm)	Interslice Gap (mm)	# Slices	Matrix	Time Scan (Min)	Nex	Flip	Angle Field of View
Locator (3 levels)	6 / 2	3	5	27	256 x 256	3-4	1	30	300
1.Axial T1 FSE MCP	716 / 12	2	2	19	512 x 512	5	2	90	120
2.Coronal T1 FSE Wrist and MCP	550 / 11	2	0	17	512 x 512	4	2	90	170
3. Coronal STIR Wrist and MCP	5116 / 29	2	0	17	512 x 512	4	2	90	170
4. Axial T1 FSE Wrist Right or Left	733 / 11	2	0	19	512 x 512	5	2	90	120
5. Coronal T1 FSE w/ Gad IV Wrist and MCP	550 / 11	2	0	17	512 x 512	4	2	90	170
6. Axial T1 FSE w/Gad IV MCP	733 / 11	2	0	19	512 x 512	5	2	90	120
7. Axial T1 FSE w/Gad IV Wrist	750 / 11	2	0	19	512 x 512	5	2	90	120

Sequences parameters for visualization from the first-through-to-fifth MCP joints and wrist of the most painful hand.
msec: milliseconds; mm: millimeters; min: minutes; MCP: metacarpal-phalanges; FSE: Fast spin echo; STIR: Short tau inversion recovery; w/Gad IV: with gadolinium intravenously (MRI Scanning Signa Twin HDx 1.5 Teslas of General Electric (GE))

We evaluated their hand-wrist bones and joints sites including distal radio-ulnar joint (1,731), identifying 964 RA known lesions (synovitis, erosions and BME/osteitis). The carpal joints were affected by synovitis more frequently than the MCP (metacarpophalanges) joints. (Table III). Wrist synovitis was present in 46% (445 site-lesions) of the patients in all three phases, erosions in 38% (362), and BME/osteitis in

TABLE III. TOTAL SITE-LESIONS IN THE 60 PATIENTS, FROM THE THREE DIFFERENT RHEUMATOID ARTHRITIS STAGES

	Synovitis n (%)	Erosion n (%)	BME n (%)
Triquetrum	54 (90.0)	56 (93.3)	25 (41.7)
Scaphoid	46 (76.7)	50 (83.3)	21 (35.0)
Lunate	40 (66.7)	43 (71.7)	24 (40.0)
Capitate	33 (55.0)	41 (68.3)	20 (33.3)
Hamate	40 (66.7)	34 (56.7)	16 (26.7)
Trapezium	42 (70.0)	28 (46.7)	10 (16.7)
Pisiform	36 (60.0)	36 (60.0)	5 (8.3)
Trapezoid	30 (50.0)	34 (56.7)	10 (16.7)
Ulnar Carpal Joint	40 (66.7)	19 (31.7)	14 (23.3)
Radio Carpal Joint	41 (68.3)	21 (35.0)	10 (16.7)
Distal Radio-Ulnar Joint	43 (71.6)	0 (0)	2 (3.3)
Total Site-Lesions 964	445 (46%)	362 (38%)	157 (16%)

n: number of sites-lesions; %: percentage within all arthritis rheumatoid (RA) stages; BME: bone marrow edema

TABLE IV. PATIENTS SITE-LESIONS IN EACH RHEUMATOID ARTHRITIS PHASE (FROM MAJOR TO MINOR FREQUENCY)

n (%)	Synovitis	CSA BME	Erosions	Synovitis	ERA BME	Erosions	Synovitis	RA BME	Erosions	m%	Total Lesions per Bone (n%)
Triquetrum	20 (87)	21 (91)	2 (9)	20 (91)	21 (96)	12 (55)	14 (93)	14 (93)	11 (73)	76.4	135 (14.0)
Scaphoid	14 (61)	16 (70)	4 (17)	18 (82)	20 (91)	10 (46)	14 (93)	14 (93)	7 (47)	66.7	117 (12.1)
Lunate	11 (48)	22 (96)	2 (9)	16 (73)	21 (96)	12 (55)	13 (87)	0 (0)	10 (67)	59.0	107 (11.1)
Capitate	10 (44)	21 (91)	4 (17)	12 (55)	20 (91)	7 (32)	11 (73)	0 (0)	9 (60)	51.4	94 (9.8)
Hamate	11 (48)	13 (57)	4 (17)	16 (73)	12 (55)	6 (27)	13 (87)	9 (60)	6 (40)	51.6	90 (9.3)
Trapezium	15 (65)	5 (22)	2 (9)	16 (73)	14 (64)	3 (14)	11 (73)	9 (60)	5 (33)	45.9	80 (8.3)
Pisiform	14 (61)	14 (61)	0 (0)	14 (64)	14 (64)	5 (23)	8 (53)	8 (53)	0 (0)	42.1	77 (8.0)
Trapezoid	10 (44)	9 (39)	0 (0)	11 (50)	14 (64)	5 (23)	9 (60)	11 (73)	5 (33)	42.9	74 (7.7)
Ulnocarpal Joint	0 (44)	3 (13)	1 (4)	19 (86)	10 (46)	8 (36)	11 (73)	6 (40)	5 (33)	41.6	73 (7.6)
Radiocarpal Joint	11 (48)	6 (26)	0 (0)	21 (96)	8 (36)	5 (23)	9 (60)	7 (47)	5(33)	41.0	72 (7.5)
Distal Radioulnar joint	11 (48)	0 (0)	2 (9)	18 (82)	0 (0)	0 (0)	14 (93)	0 (0)	0(0)	25.7	45 (4.6)

n: 60 patients; (%): percentage in the RA stage of clinically suspicious arthralgia (CSA), early rheumatoid arthrtitis (ERA) and rheumatoid arthrtitis (RA); m%: total mean percentage of lesions in each bone; in overall 964 lesions there are synovitis n = 445 (46%), erosions n = 362 (38%), BME (osteitis) n = 157 (16%)

16% (157). The triquetral bone was the most frequently affected 76.4% (135 site-lesions) with synovitis in 90% (54/60) of patients, erosions in 93.3% (56/60), and osteitis 41.7% (25/60). The scaphoid was the second most affected 66.7% (117 site-lesions) with synovitis in 76.7% (46/60), erosions in 71.7% (43/60), and osteitis 35% (21/60) of patients. (Table III & Table IV), (Figure 1, Figure 2, Figure 3).

In the inferential analysis we only found significant difference at the Pearson chi-square test ($p< 0.034$),

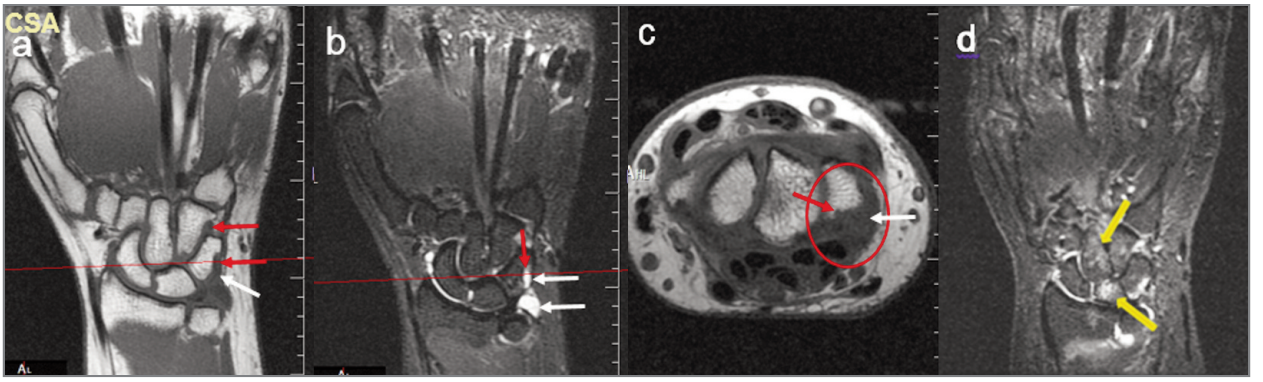

FIGURE 1. Hand-wrist MRI Coronal T1 and STIR in a clinically suspicious arthralgia (CSA) patient. First Carpal line lesions in a 59 year-old woman diagnosed with CSA. White arrows show synovitis in triquetrum bone; red arrow shows erosion in trapezoid; yellow arrows show bone marrow edema (osteitis) in hamate and scaphoid bones. **A)** T1 sequence synovitis in triquetrum and prestyloid--triquetral recess is seen hypointense (dark gray signal) (white arrow); erosions in triquetral and trapezoid cortical bones edge that usually show "no signal" (black signal), are seen hypointense in T1 due to joint effusion sinovitis (red arrow). **B)** STIR sequence synovitis in triquetrum and prestyloid-triquetral joint recess is seen hyperintense (bright white signal) (white arrow); erosion in triquetrum due to effusion synovitis within it (red arrow). **C)** T1 axial slice (corresponding to the red line level in the coronal plane), synovitis in the triquetrum is seen hypointense (white arrow in red circle) and the erosion is seen hypointense (red arrow); **D)** BME/osteitis is seen hyperintense on STIR in lunate and capitate bones (yellow arrow).

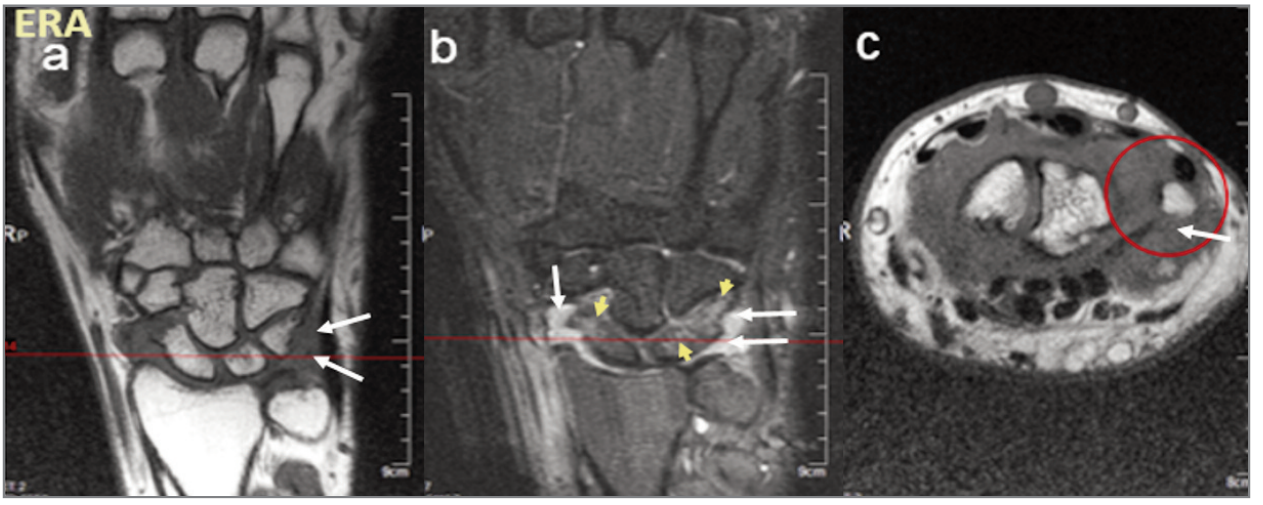

FIGURE 2. Hand-wrist MRI Coronal T1 and STIR in a early rheumatoid arthritis (ERA) patient. First Carpal line lesions in a 35 year-old man diagnosed with ERA. White arrows show synovitis; yellow arrows show bone marrow edema (osteitis). **A)** T1 sequence synovitis in triquetrum and prestyloid-triquetral recess is seen hypointense (dark gray signal) (white arrow). **B)** STIR sequence synovitis is seen hyperintense (bright white signal) in triquetrum and prestyloid-triquetral joint recess and radio-scaphoid-trapezoid joint (white arrows); BME/osteitis is seen as hyperintense signal in triquetrum, lunate and scaphoid bones (yellow arrow heads); **C)** T1 axial slice (corresponding to the red line level in the coronal plane), joint effusion synovitis triquetrum is seen hypointense (white arrow)

from presence of synovitis in all phases, dependent of the triquetral bone.

DISCUSSION

The timely diagnosis in patients with arthralgia suspected of developing RA, is an essential objective to allow the benefit of optimum treatment and improve prognosis[2,20]. Our study, based on a balanced Mexican population including three different RA stages according the ACR-EULAR criteria (2010) and EULAR-OMERACT RAMRI score reference image atlas, provides an important strength, in which, the un-reported

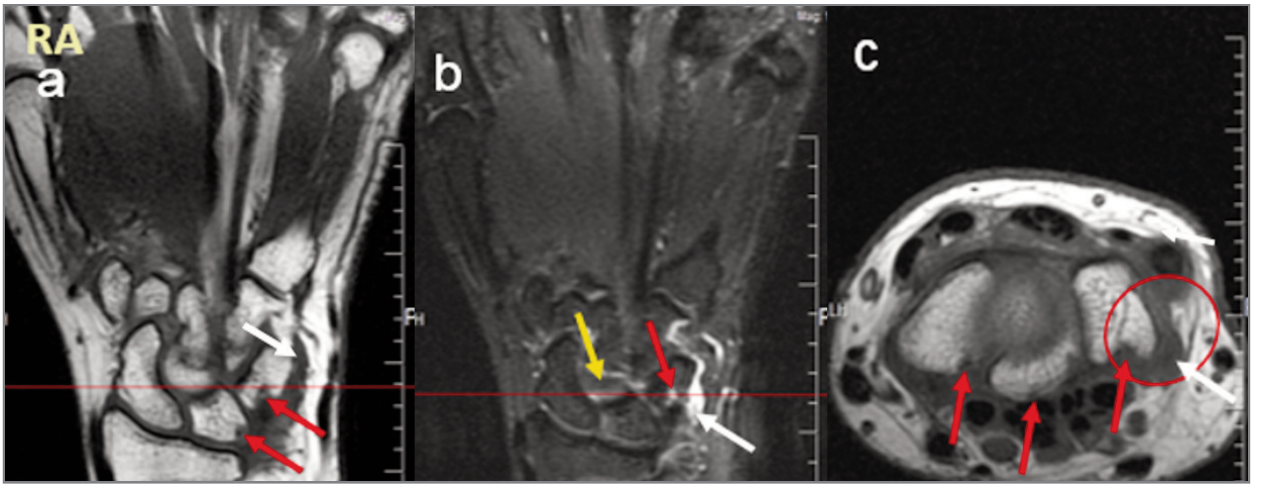

FIGURE 3. Hand-wrist MRI Coronal T1 and STIR in a rheumatoid arthritis (RA) patient. First Carpal line lesions in a 45 year-old woman. White arrows show synovitis; red arrow shows erosion; yellow arrows show bone marrow edema (osteitis). **A)** T1 sequence synovitis in triquetrum is seen hypointense (white arrow) and erosions are seen in the triquetrum, lunate and scaphoid bones edge with "no signal" (black signal), here seen hypointense in T1 due to joint effusion synovitis (red arrows). **B)** Synovitis on STIR sequence is seen hyperintense (bright white signal) in the triquetrum and prestyloid-triquetrum joint recess (white arrow); erosion in triquetrum is seen hyperintense with synovitis (red arrow); BME/osteitis is seen hyperintense in the capitate bone (yellow arrow). **C)** T1 axial slice, hypointense synovitis in prestyloid-triquetral joint recess (white arrow in red circle) and erosions with synovitis inside them, are seen hypointense in the triquetral, lunate and scaphoid bones (red arrow).

finding was obtained, regarding the predominance of triquetral bone lesion, present in 76.4% of all site-lesions in the three stages; that in the CSA stage (not previously reported in literature) reached 62.3%, followed by the lunate (51%) and scaphoid (49.3%); in ERA stage the triquetrum, lunate and scaphoid were the most prevalent sites affected with 80.6%, 74.6%, and 73% respectively, and similarly in establish RA with 86.3%, 77.6% and 51.3% for the triquetrum, scaphoid and lunate (Table IV).

This triquetral bone affectation may be due to the different ligamentous relationships as well as morphological factors, that allows rotational mobility and that pivots over the rest of the carpal bones maintaining physiological loads in the medial column wrist arch mobility. It also has the largest number of ligamentous insertions, compared to the other carpal bones, which triggers initial damage with an inflammatory process in this area[4,9] (Table I).

Patients with triquetral synovitis and erosion were also high in CSA phase, 87% and 91% respectively. It could be suggested that this higher prevalence is in relation with the major amount of ligaments and osteomyoarticular system inserted on triquetral bone, that allows it to be the pivot of the rotational mobility, loads and resistance over the rest of the carpal structures[12,21]. The scaphoid and lunate bones were the next most frequently affected bones overall, affected in 66.7% and 59% of patients respectively (Table IV).

This triquetral injury prevalence is probably influenced by its instability, since it does not directly articulate to the ulnar bone due to the presence of the triangular fibrocartilage of the wrist, which absorbs and transmits the pressure forces exerted on the carpal bones[12,13]. It has a higher tendency for traumatic injuries since it's the second one in carpal fractures frequency (38%), and represents 3-4% of all the carpal bone lesions[22-25].

There are also other factors to consider like the expected degenerative cortical bone changes by age. Miki[8] (1978) reported the articular disc wrist presents major ulnar damage at triangular cartilage level and at the interosseous ligaments between scaphoid, lunate or triquetral bones when AR begins at an early age[8]. Similarly, we found lesions in all carpal bones, most predominantly in the triquetral and lunate. The triquetral bone is probably the first and most affected due to the mechanical forces, and possibly a lower blood vessel density[4,26].

Our study included CSA, ERA, and RA stages in patients at the time of evaluation for wrist morphological changes with MRI. We report different types of lesions (synovitis, erosions, and BME/osteitis) at different sites,

making it more detailed than previously published papers[4,10,17,19,27]. A total of 23 MRI cases of patients with CSA were included, which has not been reported before. However, a limitation is the overall sample size of patients included.

CONCLUSIONS

Carpal synovitis was the most frequent lesion in all three RA phases, and the triquetrum bone the most affected. Triquetrum evaluation could be taken into account as a candidate and possible clinical biomarker of RA from its initial stages or when an initial evaluation of the disease is performed. It could be assessed as a first joint site for lesions in RA's natural history (this due to its anatomical-topographic characteristics). Nevertheless, it is necessary to perform further studies in order to obtain greater evidence for this finding. Limitations of the present study are the relatively small number of patients evaluated in each phase and that the treatment variability was not controlled, therefore that might influence on the MRI findings.

CORRESPONDENCE TO
Rodrigo Enrique Elizondo-Omaña
Av Francisco I. Madero S/N
E-mail: rod_omana@yahoo.com

REFERENCES

1. Ruiz-Esquide V, Sanmartí R. Tobacco and other environmental risk factors in rheumatoid arthritis. Reumatol Clin 2012; 8:342–350.
2. Combe B, Landewe R, Daien CI, Hua C, Aletaha D, Álvaro-Gracia JM, et al. 2016 update of the EULAR recommendations for the management of early arthritis. Ann Rheum Dis 2017; 76:948–959.
3. Erol AM, Ceceli E, Ramadan US, Borman P. Effect of rheumatoid arthritis on strength, dexterity, coordination and functional status of the hand: relationship with magnetic resonance imaging findings. Acta Reumatol Port 2016; 41:328–337.
4. Ringler MD, Murthy NS. MR imaging of wrist ligaments. Magn Reson Imaging Clin N Am 2015; 23:367–391.
5. Conaghan P, Bird P, Ejbjerg B, O'connor P, Peterfy C, McQueen F, Østergaard M. The EULAR–OMERACT rheumatoid arthritis MRI reference image atlas: the metacarpophalangeal joints. Annals of the rheumatic diseases 2005; 64 (suppl 1): i11-i21.
6. Ejbjerg B, McQueen F, Lassere M, Haavardsholm E, Conaghan P, O'connor P, Genant, H. The EULAR–OMERACT rheumatoid arthritis MRI reference image atlas: the wrist joint. Annals of the rheumatic diseases 2005; 64 (suppl 1): i23-i47.
7. Bird P, Conaghan P, Ejbjerg B, McQueen F, Lassere M, Peterfy C, Emery P. The development of the EULAR–OMERACT rheumatoid arthritis MRI reference image atlas. Annals of the rheumatic diseases 2005; 64 (suppl 1): i8-i10.
8. Miki ZD. Age changes in the triangular fibrocartilage of the wrist joint. J Anat 1978; 126:367–384.
9. Resnick D. Early abnormalities of pisiform and triquetrum in rheumatoid arthritis. Ann Rheum Dis 1976; 35:46–50.
10. Garcia-Elias M, Puig de la Bellacasa I, Schouten C. Carpal ligaments: a functional classification. Hand Clin 2017; 33:511–520.
11. Spina JC, Dutruel S, Colombo O, Badano F, Aliaga L, Barreira JC. Evaluación del daño estructural de manos mediante RM en pacientes con artritis reumatoidea temprana, sin evidencia de erosiones radiográficas. Rev argent radiol 2009; 73:439–448.
12. Medina Gonzalez CE, Benet Rodríguez M, Martínez FM. El complejo articular de la muñeca: aspectos anatofisiológicos y biomecánicos, características, clasificación y tratamiento de la fractura distal del radio. MediSur 2016; 14:430–446.
13. Totterman S, Miller R, Wasserman B, Blebea JS, Rubens DJ. Intrinsic and extrinsic carpal ligaments: evaluation by three-dimensional fourier transform mr imaging. Am J Roentgenol 1993; 160:117–123.
14. Nozaki T, Wu W Der, Kaneko Y, Rafijah G, Yang L, Hitt D, et al. High-resolution mri of the ulnar and radial collateral ligaments of the wrist. Acta radiol 2017; 58:1493–1499.
15. Lisbona MP, Maymó J. Magnetic resonance of the hand in rheumatoid arthritis. review of methodology, and its use in diagnosis, monitoring and prognosis. Reum Clin 2007; 3:126-136.
16. Boutry N, Larde A, Lapegue F, Solau-Gervais E, Flipo R, Cotten A. Magnetic resonance imaging appearance of the hands and feet in patients with early rheumatoid arthritis. J Rheumatol 2003; 30:671–679.
17. Lee KA, Min SH, Kim TH, Lee SH, Kim HR. Magnetic resonance imaging-assessed synovial and bone changes in hand and wrist joints of rheumatoid arthritis patients. The Korean journal of internal medicine 2017.
18. Tamai M, Kawakami A, Uetani M, Takao S, Tanaka F, Fujikawa K, et al. Bone edema determined by magnetic resonance imaging reflects severe disease status in patients with early-stage rheumatoid arthritis. J Rheumatol 2007; 34:2154–2157.
19. van Steenbergen HW, Mangnus L, Reijnierse M, Huizinga TWJ, van der Helm-van Mil AHM. Clinical factors, anticitrullinated peptide antibodies and mri-detected subclinical inflammation in relation to progression from clinically suspect arthralgia to arthritis. Ann Rheum Dis 2016; 75:1824–1830.
20. Arana-Guajardo A, Pérez-Barbosa L, Vega-Morales D, Riega-Torres J, Esquivel-Valerio J, Garza-Elizondo M. Aplicación de un modelo de predicción de progresión de artritis reumatoide en pacientes con artritis indiferenciada. Reumatol Clínica 2014; 10:360–363.
21. Østergaard M, Peterfy C, Conaghan P, McQueen F, Bird P, Ejbjerg B, et al. OMERACT rheumatoid arthritis magnetic resonance imaging studies. core set of mri acquisitions, joint pathology definitions, and the OMERACT RA-MRI scoring system. J Rheumatol 2003; 30:1385–1386.
22. Paruchuri RK, Rajasekhar L, Reddy VS. Role of mri in evaluation of asymmetric undifferentiated hand arthritis [Letter]. Indian J Rheumatol 2016; 11:60–61.
23. van Steenbergen HW, Aletaha D, Beaart-van de Voorde LJJ, Brouwer E, Codreanu C, Combe B, et al. EULAR definition of arthralgia suspicious for progression to rheumatoid arthritis. Ann Rheum Dis 2017; 76:491–496.
24. Díez Renovales F, Nates Uribe N, Korta I, Sarmiento de la Iglesia MM, Galíndez Agirregoikoa E, Grande Icaran D. Utilidad de la RM en la valoración de la AR. Estado actual. [Review]. Radiologia 2014; 56:871.
25. Narváez García JA. Valoración por imagen de la artritis reumatoide precoz. Reumatol Clin 2010; 6:111–114.
26. Daunt N. Magnetic resonance imaging of the wrist: anatomy and pathology of interosseous ligaments and the triangular fibrocartilage complex. Curr Probl Diagn Radiol 2002; 31:158–76.
27. Honing EW, Moeller JL. Wrist Injuries. Phys Sportsmed1998; 26:40–49.